

Determination of rheological properties of whole blood with a scanning capillary-tube rheometer using constitutive models[†]

Sangho Kim¹, Bumseok Namgung¹, Peng Kai Ong¹, Young I. Cho²,
Keyoung Jin Chun³ and Dohyung Lim^{3,*}

¹*Division of Bioengineering and Department of Surgery, National University of Singapore, Singapore 117574, Singapore*

²*Department of Mechanical Engineering & Mechanics, Drexel University, Philadelphia, PA 19104, USA*

³*Gerontechnology Center, Korea Institute of Industrial Technology, Chungnam, 330-825, Korea*

(Manuscript Received December 9, 2008; Revised February 5, 2009; Accepted March 12, 2009)

Abstract

We examine the applicability of three different non-Newtonian constitutive models (power-law, Casson, and Herschel-Bulkley models) to the determination of blood viscosity and yield stress with a scanning capillary-tube rheometer. For a Newtonian fluid (distilled water), all three models produced excellent viscosity results, and the measured values of the yield stress with each model were zero. For unadulterated human blood, the Casson and Herschel-Bulkley models produced much stronger shear-thinning viscosity results than the power-law model. The yield stress values for the human blood obtained with the Casson and Herschel-Bulkley models were 13.8 and 17.5 mPa, respectively. The two models showed a small discrepancy in the yield stress values, but with the current data analysis method for the scanning capillary-tube rheometer, the Casson model seemed to be more suitable in determining the yield stress of blood than the Herschel-Bulkley model.

Keywords: Blood viscosity; Yield stress; Power-law; Casson; Herschel-Bulkley

1. Introduction

The flow properties of the blood are affected by a number of factors, which include hematocrit (volume fraction of red blood cells in whole blood), plasma viscosity, red blood cell aggregation, and deformability. Furthermore, the viscosity of blood is non-Newtonian, which increases as shear rate (velocity gradient in a flowing material) decreases. Hematocrit is one of the major factors determining the blood viscosity at high shear rates while red blood cell aggregation plays a significant role at low shear rates. At normal hematocrit concentrations (35-45%), red blood cell deformability may affect blood viscosity and becomes a major factor in the microcirculation.

Recently, a new U-shaped scanning capillary-tube rheometer (SCTR) has been developed from the concept of the conventional capillary-tube viscometer [1-4]. The rheometer is capable of measuring whole blood viscosity continuously over a wide range of shear rates without adding any anticoagulants. However, there are some limitations in using the SCTR for viscosity measurements of fluids. Since the device utilizes charge-coupled devices and light-emitting diode arrays to determine liquid-height changes over time, viscosity of transparent liquids cannot be measured [1]. Another major limitation of using this new device for liquid viscosity measurements lies in the selection of constitutive models. The SCTR was developed specially for blood viscosity and yield stress measurements using the Casson model [2]. However, many earlier studies report that not only the Casson model but also other non-Newtonian constitutive models effectively describe blood flows in biological

[†] This paper was recommended for publication in revised form by Associate Editor Gihun Son

*Corresponding author. Tel.: +82 41 589 8428, Fax.: +82 41 589 8420

E-mail address: dli349@gmail.com

© KSME & Springer 2009

systems. For instance, Bingham plastic, Casson, and Herschel-Bulkley (H-B) models were used to describe the rheological behavior of yield-stress fluids [5]. Picart et al. [6] used the value of the shear stress at a shear rate of 10^{-3} s^{-1} as a measure of the yield stress in their report. In a study by Barnes [7], the H-B model described reasonably well the data reported by Picart and coworkers.

Table 1 shows three non-Newtonian constitutive models (power-law, Casson, and H-B models) that have been used by a number of researchers for investigating blood rheology and flows. Siau et al. [9] performed a comparative study of the power-law and Casson models for prediction of unsteady stenosis flows, whereas Tu and Deville [10] used H-B, Bingham, and power-law models for their study on stenosis flows. It has been pointed out that the selection of constitutive model may significantly affect the analysis of blood flows [9, 10].

The main purpose of the present study is to examine whether the results of blood rheology and flow obtained with the current data analysis method for the SCTR are significantly altered by the choice of constitutive model. Hence, the study investigated the effect of constitutive model selection on the blood viscosity and yield stress measurements and prediction of blood flow patterns using the SCTR. It is well known that human blood has both shear-thinning characteristics and yield stress, which make the blood viscosity increase with decreasing shear rate. We examined the capability of three constitutive models in handling data obtained with the SCTR for determinations of blood viscosity and yield stress. The power-law model was chosen to address the shear-thinning behavior of blood. The Casson and H-B models were selected to address both the shear-thinning viscosity and yield stress of blood.

2. Materials and methods

The experimental preparation and data acquisition methods have been described previously [2, 3], and the reader is referred to those studies for a complete description. Viscosity values of distilled water and unadulterated human blood were determined with the scanning capillary-tube rheometer (SCTR) over a wide range of shear rates. Human blood was obtained from a healthy male donor aged 29. Venous blood sample $\sim 3 \text{ ml}$ was withdrawn and directly transferred into a disposable capillary-tube set in the SCTR for

Table 1. Various physiological studies with non-Newtonian constitutive models.

Researchers	Power-law	Casson	Herschel-Bulkley
Chakravarty and Datta [8]	x		x
Siau et al. [9]	x	x	
Tu and Deville [10]	x		x
Liepsch and Moravec [11]	x		
Rohlf and Tenti [12]		x	
Misra et al. [13, 14]		x	
Das and Batra [15]		x	
Dash et al. [16]		x	
Misra and Kar [17]			x
Chakravarty and Datta [18, 19]			x

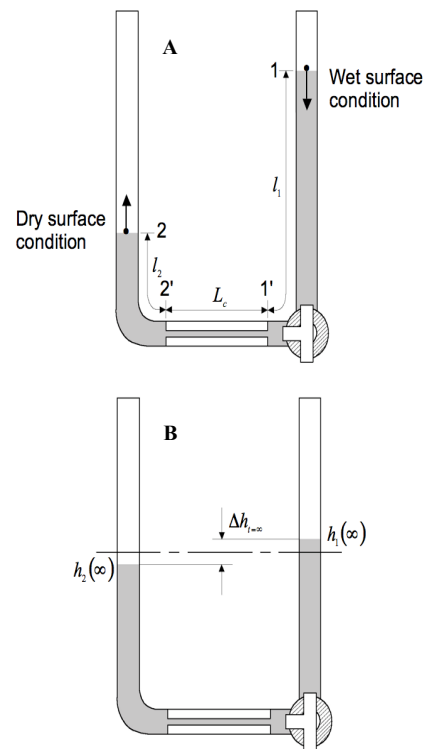


Fig. 1. Liquid-solid interface condition for each vertical tube of a U-shaped scanning capillary tube rheometer.

viscosity and yield stress determinations. The length and inner diameter of the capillary tube used in this study were 100 and 0.797 mm, respectively. Fluid height changes with time in the riser tubes shown in

Fig. 1 were measured with an accuracy of 0.083 mm. Human blood was examined at a body temperature of 37°C, while tests with distilled water were performed at a room temperature of 25°C.

2.1 Surface tension and yield stress

Fig. 1A shows that the fluid level in the right-side vertical tube (riser tube 1) decreases while that in the left-side vertical tube (riser tube 2) increases. Even when time goes to infinity (i.e., $t \sim 3$ minutes), the two fluid levels do not become equal due to any differences in surface tension and yield stress at the two riser tubes (see Δh_{∞} in Fig. 1B). As shown in Fig. 1A, the riser tube 1 always has a fully wet surface condition, whereas the riser tube 2 has an almost perfectly dry surface condition during the entire test. Therefore, the surface tension at the riser tube 1 is consistently greater than that at the riser tube 2 [2].

The time-dependent flow in the SCTR is analyzed to determine the viscosities of distilled water and whole blood. Assuming a quasi-steady flow, the governing equation can be simplified as follows:

$$\Delta P_c(t) = \rho g [h_1(t) - h_2(t) - \Delta h_{st}] \quad (1)$$

where $\Delta P_c(t)$ is the pressure drop across the capillary tube, ρ is the density of fluid, g is gravitational acceleration, $h_1(t)$ and $h_2(t)$ are fluid levels at the riser tubes 1 and 2, respectively, Δh_{st} is a constant representing the additional height difference due to the surface tension, and t is the time from the start of experiment. The detailed mathematical derivation is shown in the Appendix.

2.2 Power-law model

A typical flow curve obtained with the power-law model indicates that the ratio of shear stress to shear rate, often called apparent viscosity, falls progressively with increasing shear rate. The viscosity for a power-law fluid can be expressed as follows:

$$\eta = m\dot{\gamma}^{n-1} \quad (2)$$

where η is the apparent viscosity, m and n are power-law model constants, and $\dot{\gamma}$ is shear rate. The constant, m , is a measure of the consistency of the fluid: the higher the m is, the more viscous the fluid is. n is a measure of the degree of non-Newtonian behavior: the greater the departure from the unity is,

the more pronounced the non-Newtonian properties of the fluid are. The mathematical details of curve-fitting procedure to determine the two unknowns, m and n , in the SCTR were reported in our previous study [3]. The velocity profile in the capillary tube (V_c) can be expressed by the following equation:

$$V_c(t, r) = \left(\frac{n}{n+1} \right) \cdot \left(\frac{\rho g [h_1(t) - h_2(t) - \Delta h_{st}]}{2mL_c} \right)^{\frac{1}{n}} \cdot \left(R_c^{\frac{n+1}{n}} - r^{\frac{n+1}{n}} \right) \quad (3)$$

where R_c and L_c are the radius and length of the capillary tube, respectively. Note that when the power-law index, n , becomes 1, the above equation yields to the Newtonian velocity profile.

2.3 Casson model

The Casson model mathematically describes the shear-thinning characteristics of blood viscosity with a yield stress term:

$$\sqrt{\tau} = \sqrt{\tau_y} + \sqrt{k} \sqrt{\dot{\gamma}} \quad \text{when } \tau \geq \tau_y \quad (4a)$$

$$\dot{\gamma} = 0 \quad \text{when } \tau \leq \tau_y \quad (4b)$$

where τ_y is a constant that is interpreted as the yield stress, and k is a Casson model constant.

The velocity profile at the capillary tube can be obtained by integration of shear rate using the Casson model as follows:

$$V_c(t, r) = \frac{R_c^2 \Delta P_c(t)}{4kL_c} \times \left[1 - C^2(r) - \frac{8}{3} C_y^{\frac{1}{2}}(t) \left\{ 1 - C^{\frac{3}{2}}(r) \right\} + 2C_y(t)(1 - C(r)) \right] \quad \text{for } r_y(t) \leq r \leq R_c \quad (5a)$$

$$V_c(t) = \frac{R_c^2 \Delta P_c(t)}{4kL_c} (1 - \sqrt{C_y(t)})^3 \cdot \left(1 + \frac{1}{3} \sqrt{C_y(t)} \right) \quad \text{for } r_y(t) \geq r \quad (5b)$$

where $C(r) = \frac{r}{R_c}$ and

$$C_y(t) = \frac{r_y(t)}{R_c} = \frac{\tau_y}{\tau_w(t)} = \frac{\Delta h_y}{h_1(t) - h_2(t) - \Delta h_{st}}$$

Note that $r_y(t)$ is the radial position where shear stress becomes equal to the yield stress. Thus, where

$r \leq r_y$, the velocity profile becomes blunted.

The data reduction procedure to determine the unknowns (k , Δh_{st} , and Δh_y) was reported in our recent study [2]. Once the unknowns are determined, the apparent viscosity can be expressed in terms of the wall shear rate as follows:

$$\eta_w(t) = k + \frac{\tau_y}{\dot{\gamma}_w(t)} + \frac{\sqrt{4k\tau_y}}{\sqrt{\dot{\gamma}_w(t)}} \tag{6}$$

$$= k + \frac{\left(\frac{\rho g R_c \Delta h_y}{2L_c}\right)}{\dot{\gamma}_w(t)} + \frac{\sqrt{2k\rho g R_c \Delta h_y}}{\sqrt{\dot{\gamma}_w(t) L_c}}$$

The yield stress for the Casson model can be calculated by using the following equation, which is also applicable to Herschel-Bulkley model as well.

$$\tau_y = \frac{\rho g \Delta h_y \cdot R_c}{2L_c} \tag{7}$$

2.4 Herschel-Bulkley (H-B) model

The Herschel-Bulkley (H-B) model is described as follows:

$$\tau = m\dot{\gamma}^n + \tau_y \quad \text{when } \tau \geq \tau_y \tag{8a}$$

$$\dot{\gamma} = 0 \quad \text{when } \tau \leq \tau_y \tag{8b}$$

where τ_y is the yield stress, and m and n are the H-B model constants. Since the H-B model reduces to the power-law model when a fluid does not have a yield stress, this model can be considered to be more general than the Casson model that reduces to a Newtonian model when τ_y becomes zero.

The expression of the shear rate outside the plug-flow region at the capillary tube can be obtained from the H-B model as follows:

$$\dot{\gamma} = -\frac{dV_c}{dr} = \left(\frac{\Delta P_c}{2mL_c}\right)^{\frac{1}{n}} (r - r_y)^{\frac{1}{n}} \tag{9}$$

for $r_y(t) \leq r \leq R_c$

where $r_y(t)$ is a radial location below which the velocity profile is uniform due to yield stress, i.e., plug flow. Using Eq. (9), the velocity profile at the capillary tube is expressed as follows:

$$V_c(t, r) = \left(\frac{n}{n+1}\right) \cdot \left(\frac{R_c^{n+1} \Delta P_c(t)}{2mL_c}\right)^{\frac{1}{n}} \left\{ \left(1 - C_y(t)\right)^{\frac{n+1}{n}} - \left(C(r) - C_y(t)\right)^{\frac{n+1}{n}} \right\} \tag{10a}$$

for $r_y(t) \leq r \leq R_c$

$$V_c(t) = \left(\frac{n}{n+1}\right) \cdot \left(\frac{R_c^{n+1} \Delta P_c(t)}{2mL_c}\right)^{\frac{1}{n}} \cdot \left(1 - C_y(t)\right)^{\frac{n+1}{n}} \tag{10b}$$

for $r_y(t) \geq r$

where $C(r)$ and $C_y(t)$ are identical to those described in Eq. (5).

To determine the mean flow velocity at a riser tube, one needs to analytically derive the expression of the flow rate at the capillary tube first. Volume flow rate can be obtained by integrating the velocity profile over the cross-sectional area of the capillary tube, and the mean flow velocity at the vertical tube, $\bar{V}_r(t)$, can be derived using the flow rate as follows:

$$\bar{V}_r(t) = \frac{R_c^{\frac{3n+1}{n}}}{R_c^2} \left(\frac{n}{n+1}\right) \cdot \left(\frac{\rho g [h_1(t) - h_2(t) - \Delta h_{st}]}{2kL_c}\right)^{\frac{1}{n}} \times \left[\left(\frac{\Delta h_y}{h_1(t) - h_2(t) - \Delta h_{st}}\right)^2 \cdot \left(1 - \frac{\Delta h_y}{h_1(t) - h_2(t) - \Delta h_{st}}\right)^{\frac{n+1}{n}} + \left(1 + \frac{\Delta h_y}{h_1(t) - h_2(t) - \Delta h_{st}}\right) \cdot \left(1 - \frac{\Delta h_y}{h_1(t) - h_2(t) - \Delta h_{st}}\right)^{\frac{2n+1}{n}} - 2 \left(\frac{n}{2n+1}\right) \cdot \left(\frac{\Delta h_y}{h_1(t) - h_2(t) - \Delta h_{st}}\right) \cdot \left(1 - \frac{\Delta h_y}{h_1(t) - h_2(t) - \Delta h_{st}}\right)^{\frac{2n+1}{n}} - 2 \left(\frac{n}{3n+1}\right) \cdot \left(1 - \frac{\Delta h_y}{h_1(t) - h_2(t) - \Delta h_{st}}\right)^{\frac{3n+1}{n}} \right] \tag{11}$$

There are four unknown parameters to be determined through the curve fitting in Eq. (11): Δh_{st} , m , n , and Δh_y . The curve-fitting method [2] used for the Casson model was applied to determine the unknown parameters from the experimental values of $h_1(t)$ and $h_2(t)$.

The apparent viscosity can be expressed in terms of the wall shear rate as follows:

$$\eta_w(t) = m\dot{\gamma}_w(t)^{n-1} + \frac{\tau_y}{\dot{\gamma}_w(t)} + \frac{\left(\frac{\rho g R_c \Delta h_y}{2L_c}\right)}{\dot{\gamma}_w(t)} \tag{12}$$

where m , n , and τ_y are the properties of blood to be determined using the H-B model. Note that when n becomes 1, the mathematical form of the H-B model yields to Bingham plastic model.

3. Results and discussions

Fig. 2A shows viscosity results for distilled water at 25°C obtained with the scanning capillary-tube rheometer (SCTR) using the three different non-Newtonian constitutive models for comparison. The values of Δh_{cr} were approximately 3.3–3.4 mm for the three models, whereas the values of Δh_y were determined to be zero for all models, validating capability of the data reduction method to deal with any fluids regardless of yield stress existence. The viscosity of distilled water was found to be between 0.884 and 0.905 cP at 25°C for all three models. The test results obtained with the SCTR gave less than 2% error compared with the reference data (0.892 cP). Fig. 2B shows test results of fresh, unadulterated human blood at a body temperature of 37°C. The test was completed within 3 minutes to avoid blood clotting, which might have affected the viscosity and yield stress determinations. The hematocrit of this donor's blood was 42%. The power-law model showed relatively low viscosity data at low shear rates compared with the Casson and H-B models. However, the viscosity data determined with the all three constitutive models were in a good agreement at high shear rates.

Figs. 3A and 3B show the results of shear stress versus shear rate for distilled water and human blood, respectively. In the case of distilled water, the shear stress obtained with the three non-Newtonian models was almost identical over the entire range of shear rates. The yield stress can be graphically described as the intersecting point where the shear stress curve meets with the y-axis (i.e., at zero shear rate). Table 2 shows values of the yield stress together with the model constants of the three constitutive models. As expected, the distilled water shows no yield stress, while human blood shows finite values of the yield stress for the cases of Casson and H-B models. The yield stress values of human blood with hematocrit of 42% were 13.8 and 17.5 mPa for the Casson and H-B models, respectively. Based on studies by Picart et al. [6], the yield stress values vary from 1 to 30 mPa for normal human blood with hematocrit of 40%, which supports the present method of yield stress determination using the SCTR. The surface roughness of the

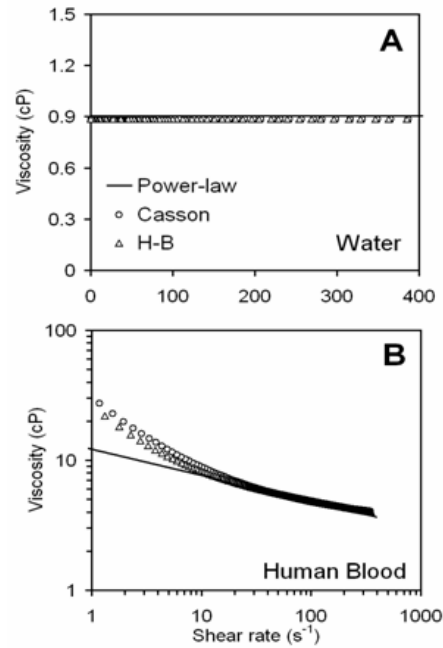


Fig. 2. Viscosity results obtained with a scanning capillary tube rheometer. (A) Distilled water at 25°C. (B) Unadulterated human blood at 37°C. Note that viscosity data of human blood are shown in a log-log scale.

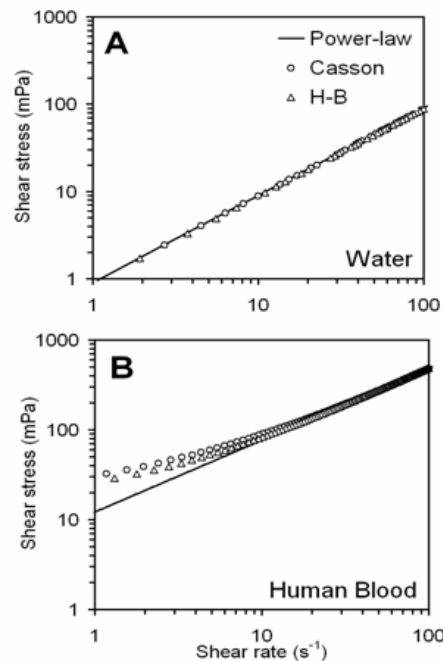


Fig. 3. Wall shear stress vs. shear rate in a capillary tube. (A) Distilled water at 25°C. (B) Unadulterated human blood at 37°C. Note that all data shown here are in a log-log scale.

Table 2. Comparison of model constants, Δh_y , and τ_y .

	Power-law	H-B	Casson
Distilled Water (25°C)	$n = 1$ $m = 0.905$	$n = 1$ $m = 0.884$	$k = 0.886$ cP
	$\Delta h_y = 0.00$	$\Delta h_y = 0.00$	$\Delta h_y = 0.00$
	$\tau_y = 0.0$	$\tau_y = 0.0$	$\tau_y = 0.0$
Human Blood (37°C)	$n = 0.799$ $m = 12.171$	$n = 0.860$ $m = 8.972$	$k = 3.290$ cP
	$\Delta h_y = 0.00$	$\Delta h_y = 0.85$ mm	$\Delta h_y = 0.67$ mm
	$\tau_y = 0.0$	$\tau_y = 17.5$ mPa	$\tau_y = 13.8$ mPa

Note that $m \equiv [\text{cP}\cdot\text{s}^{n-1}]$

capillary tube might influence the yield stress measurement of blood. For a smooth geometry like a glass tube, slip effect at the wall becomes substantial below a shear rate of 0.5 s^{-1} [6]. However, since the shear rates used in the present study are equal or greater than 1 s^{-1} , we assume that the slip effect on the blood viscosity and yield stress measurements with the SCTR is negligibly small.

The yield stress of human blood obtained with the H-B model was consistently greater than that obtained with the Casson model as shown in Table 3. To evaluate which model produces more accurate yield stress results with the current data reduction method and system, the experimentally measured values of Δh_{∞} were compared with those of $\Delta h_{st} + \Delta h_y$ determined analytically through the curve-fitting procedure for human blood (see Table 3). The experimental values (Δh_{∞}) should physically be bigger than those ($\Delta h_{st} + \Delta h_y$) obtained analytically since we assumed that the value of the fluid level difference in the riser tubes 1 and 2 at $t = 180 \text{ s}$ would be slightly bigger than but very close to the true value of Δh_{∞} . As shown in Table 3, the values of $\Delta h_{st} + \Delta h_y$ analytically calculated with the Casson model were consistently smaller than the experimentally measured values, whereas the values calculated with H-B model were larger. Based on this comparison using the current data analysis method for the SCTR, one may conclude that the Casson model does a better job in determining the yield stress of blood than the H-B model. However, it is of note that both models produced almost identical values of Δh_{st} ; thus the effect of the surface tensions was properly handled in both models for the human blood.

As shown in Fig. 4, $C_y(t)$ (plug-flow region) for human blood at the capillary tube increases with time. Due to the discrepancy in the yield stress values

Table 3. Comparison of Δh_{∞} and $\Delta h_{st} + \Delta h_y$.

		H-B	Casson
Human Blood (37°C)	Δh_{∞} (experimental)	9.13 mm	9.13 mm
	$\Delta h_{st} + \Delta h_y$ (analytical)	9.25 mm $\Delta h_{st} = 8.4$ mm $\Delta h_y = 0.85$ mm	9.07 mm $\Delta h_{st} = 8.4$ mm $\Delta h_y = 0.67$ mm

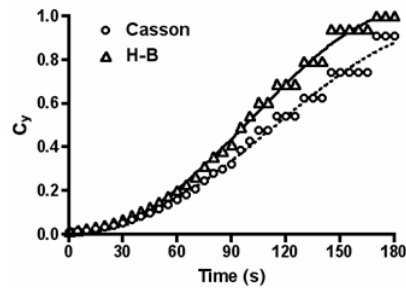


Fig. 4. Variations of a plug-flow region in a capillary tube as a function of time for human blood at 37°C. Dotted and solid lines represent 4th-order polynomial regression curves for data obtained with the Casson and Herschel-Bulkley models, respectively. For both regression results, $R^2 = 0.99$.

obtained with the Casson and H-B models, the size difference in the plug-flow region estimated from the two models became more pronounced as shear rate decreased. The yield stress of blood plays a significant role in determination of both viscosity and velocity profile in blood flow, in particular at low flow rates. It is of note that the H-B model predicts a larger plug-flow region than the Casson model. The size of the plug-flow region may significantly influence the shape of velocity profile, resulting in alteration of the wall shear rate. At a given mean velocity in the capillary tube, a plug-flow region would lead to an elevation of shear rate at the wall, which lowers apparent viscosity. To understand effects of the plug-flow region at a given flow rate on the wall shear stress, we need to consider both shear rate and viscosity since the shear stress is calculated from the product of shear rate and viscosity. Thus, the plug-flow region effect on the wall shear stress is not very clear since its two opposing effects on shear rate and viscosity may cancel one another out, resulting in a small alteration in the wall shear stress. The wall shear stress in small arteries and arterioles is an important factor in clinical hemorheology as it is one of the principal stimuli for release of the vasodilators including nitric oxide and prostaglandins by endothelial cells [20, 21]. Therefore, model constants and the method of determining blood

viscosity and yield stress in this study, combined with clinical use of the SCTR, would be useful in the diagnosis and treatment of cardiovascular diseases [22].

4. Conclusions

The present study investigated the applicability of three non-Newtonian constitutive models (power-law, Casson, and Herschel-Bulkley (H-B) models) on the measurements of fluid viscosity and yield stress using a scanning capillary-tube rheometer (SCTR). For a Newtonian fluid (distilled water), all three models produced excellent viscosity results. For unadulterated human blood, both Casson and H-B models gave viscosity results which are in good agreement with each other, whereas the power-law model seemed to produce inaccurate viscosity measurements at low shear rates due to its inability to handle the yield stress of blood. The yield stress values obtained from the Casson and H-B models for the human blood were measured to be 13.8 and 17.5 mPa, respectively. The two models showed a small discrepancy in the yield-stress values. In the yield stress determination using the SCTR with the current data reduction procedure, the Casson model seemed to be more suitable than the H-B model.

Acknowledgment

This work was supported by NUS Grant R-397-000-048-133 and performed with funding from the Korea Institute of Industrial Technology (KITECH).

References

- [1] S. Kim and Y. I. Cho, Effect of dye concentration on the viscosity of water in a scanning capillary-tube viscometer, *J. Non-Newtonian Fluid Mech.*, 111 (2003) 63-68.
- [2] S. Kim, Y. I. Cho, W. N. Hogenauer and K. R. Kenney, A method of isolating surface tension and yield stress effects in a U-shaped scanning capillary-tube viscometer using a Casson model, *J. Non-Newtonian Fluid Mech.*, 103 (2002) 205-219.
- [3] S. Kim, Y. I. Cho, A. H. Jeon, B. Hogenauer and K. R. Kenney, A new method for blood viscosity measurement, *J. Non-Newtonian Fluid Mech.*, 1939 (2000) 1-10.
- [4] S. Kim, Y. I. Cho, K. R. Kenney, R. O. Pellizzari and P. R. Stark, A scanning dual-capillary-tube viscometer, *Rev. Sci. Instrum.*, 71 (2000) 3188-3192.
- [5] Q. D. Nguyen and D. V. Boger, Measuring the flow properties of yield stress fluids, *Annu. Rev. Fluid Mech.*, 24 (1992) 47.
- [6] C. Picart, J. M. Piau and H. Galliard, Human blood shear yield stress and its hematocrit dependence, *J. Rheol.*, 1 (1998) 42.
- [7] H. A. Barnes, The yield stress-a review- everything flows?, *J. Non-Newtonian Fluid Mech.*, 81 (1999) 133.
- [8] S. Chakravarty, A. Datta, Dynamic Response of stenotic blood flow in vivo, *Mathl. Comput. Modelling*, 16 (1992) 3-20.
- [9] W. L. Siau, E. Y. K. Ng and J. Mazumdar, Unsteady stenosis flow prediction: a comparative study of non-Newtonian models with operator splitting scheme, *Medical Engineering & Physics*, 22 (2000) 265-277.
- [10] C. Tu and M. Deville, Pulsatile flow of non-Newtonian fluids through arterial stenoses, *J. Biomechanics*, 29 (1996) 899-908.
- [11] D. Liepsch and S. Moravec, Pulsatile flow of non-Newtonian fluids in distensible models of human arteries, *Biorheology*, 21 (1984) 571.
- [12] K. Rohlf and G. Tenti, The role of the Womersley number in pulsatile blood flow a theoretical study of the Casson model, *J. Biomechanics*, 34 (2001) 141-148.
- [13] J. C. Misra and S. K. Ghosh, Flow of a Casson fluid in a narrow tube with a side branch, *International Journal of Engineering Science*, 38 (2000) 2045-2077.
- [14] J. C. Misra and S. K. Pandey, Peristaltic transport of blood in small vessels: Study of a mathematical model, *Computers and Mathematics with Applications*, 43 (2002) 1183-1193.
- [15] B. Das, R. L. Batra, Non-Newtonian flow of blood in an arteriosclerotic blood vessel with rigid permeable walls, *J. Theor. Biol.*, 175 (1995) 1-11.
- [16] R. K. Dash, G. Jayaraman and K. N. Mehta, Estimation of increased flow resistance in a narrow catheterized artery-A theoretical model, *J. Biomechanics*, 29 (1996) 917-930.
- [17] J. C. Misra and B. K. Kar, A mathematical analysis of blood flow from a feeding artery into a branch capillary, *Mathl. Comput. Modelling*, 15 (1991) 9-18.
- [18] S. Chakravarty and A. Datta, Effects of stenosis on arterial rheology through a mathematical model, *Mathl. Comput. Modelling*, 12 (1989) 1601-1612.

- [19] S. Chakravarty and A. Datta, Dynamic Response of arterial blood flow in the presence of multi-stenoses, *Mathl. Comput. Modelling*, 13 (1990) 37-55.
- [20] R. Busse, I. L. Megson and P. G. Wright, Diffusion of nitric oxide and scavenging by blood in the vasculature, *Biochimica et Biophysica Acta*, 1425 (1998) 168-176.
- [21] A. Koller and G. Kaley, Prostaglandins mediate arteriolar dilation to increase blood flow velocity in skeletal microcirculation. *Cir. Res.*, 67 (1990) 529-534.
- [22] S. K. Samijo, J. M. Willigers, R. Barkhuysen, P. J. E. H. M. Kitslaar, R. S. Reneman and P. J. Brands, Wall shear stress in the human common carotid artery as function of age and gender, *Cardiovascular Research*, 39 (1998) 515.

Appendix

Quasi-steady flow

The mathematical description starts with the equation of the conservation of energy in the form of pressure unit, where the surface-tension effect is considered between the top two points of the fluid columns at the vertical tubes [2]. Assuming that the surface tension for the liquid-solid interface at each vertical tube remains constant during the test, one may write the governing equation as follows:

$$\begin{aligned}
 & P_1(t) + \frac{1}{2} \rho V_1(t)^2 + \rho g h_1(t) \\
 & = P_2(t) + \frac{1}{2} \rho V_2(t)^2 + \rho g h_2(t) + \quad (A.1) \\
 & \Delta P_c(t) + \rho g \Delta h_{st} + \rho \int_{s_1}^{s_2} \frac{\partial V}{\partial t} ds
 \end{aligned}$$

where P_1 and P_2 are static pressures at the top two points (see points 1 and 2 in Fig. 1), ρ is the density of fluid, g is gravitational acceleration, $V_1(t)$ and $V_2(t)$ are flow velocities at the two vertical tubes, $h_1(t)$ and $h_2(t)$ are fluid levels at the right and left vertical tubes, respectively, $\Delta P_c(t)$ is the pressure drop across the capillary tube, Δh_{st} is a constant representing the additional height difference due to the surface tension, t is time, s is the distance measured along the streamline from some arbitrary initial point.

For the convenience of data-reduction procedure, the unsteady term in Eq. (A1),

$$\rho \int_{s_1}^{s_2} \frac{\partial V}{\partial t} ds, \text{ may be ignored under the assumption}$$

of a quasi-steady state. To make the assumption, we examined whether the pressure drop due to the unsteady effect was negligibly small compared with that due to the friction estimated from the steady *Poiseuille flow* in the capillary tube.

The unsteady term can be broken into three integrations that represent the pressure drops due to the unsteady flow along the streamlines at vertical tube 1, capillary tube, and vertical tube 2 as follows:

$$\rho \int_{s_1}^{s_2} \frac{\partial V}{\partial t} ds = \rho \left(\int_{s_1}^{s_r} \frac{d\bar{V}_r}{dt} ds + \int_{s_r}^{s_c} \frac{d\bar{V}_c}{dt} ds + \int_{s_c}^{s_2} \frac{d\bar{V}_r}{dt} ds \right) \quad (A.2)$$

where \bar{V}_r and \bar{V}_c are mean flow velocities at vertical and capillary tubes, respectively. Using the conservation of mass, $\pi R_c^2 \cdot \bar{V}_c = \pi R_r^2 \cdot \bar{V}_r$, the pressure drop due to the unsteady effect can be reduced as follows:

$$\Delta P_{unsteady} = \rho \int_{s_1}^{s_2} \frac{\partial V}{\partial t} ds = \rho \left\{ L_c \left(\frac{R_r}{R_c} \right)^2 + l_1 + l_2 \right\} \frac{d\bar{V}_r}{dt} \quad (A.3)$$

where l_1 and l_2 are lengths of the liquid columns in the vertical right and left tubes, respectively, L_c is the length of the capillary tube (see Fig. 1A), R_r and R_c are the radii of the vertical and capillary tubes, respectively.

In the present experimental set up, l_1 , l_2 , and L_c were approximately 12, 4, and 10 cm, respectively. Since $h_1(t)$ and $h_2(t)$ are governed by the conservation of mass for incompressible fluids, \bar{V}_r should be equal to $|dh_1(t)/dt|$ and $|dh_2(t)/dt|$. To calculate the term $d\bar{V}_r/dt$ from experimental values, one could use the following central differential method:

$$\begin{aligned}
 \frac{d\bar{V}_r}{dt} & = \left| \frac{[h_1(t + \Delta t) - 2h_1(t) + h_1(t - \Delta t)]}{\Delta t^2} \right| \\
 & = \left| \frac{[h_2(t + \Delta t) - 2h_2(t) + h_2(t - \Delta t)]}{\Delta t^2} \right| \quad (A.4)
 \end{aligned}$$

$\Delta P_{unsteady}$ was estimated through a curve-fitting process using a least-square method. To obtain a smooth curve from raw data, the following exponential equation was used.

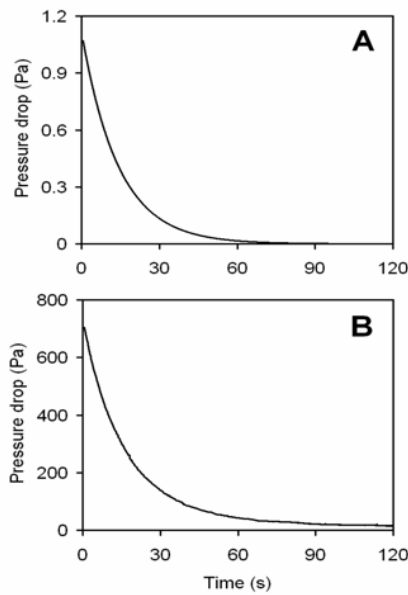


Fig. A1. Pressure drop at a capillary tube during a test with human blood. (A) Pressure drop due to an unsteady flow. (B) Pressure drop across a capillary tube due to viscous friction.

$$Error = \left(\frac{d\bar{V}_r}{dt} - a \cdot e^{-bt} \right)^2 \quad (A.5)$$

where the sum of the error was minimized to determine two constants, a and b , for all 11,000 data points obtained in each test.

As shown in Fig. A1, the pressure drop due to the unsteady effect was much smaller than that due to the viscous friction at the capillary tube. Typically, the pressure drop attributable to the unsteady effect (A) was less than 1.2 Pa, while the pressure drop due to the friction (B) at the capillary tube was greater than 700 Pa at the beginning of a test. Furthermore, the pressure drop caused by the unsteady flow (A) was always less than 1% of the pressure drop due to the

viscous friction (B) over the entire shear-rate range. This confirms that the assumption of a quasi-steady state can be used for the present data reduction procedure. Assuming a quasi-steady flow behavior, Eq. (A1) can be simplified as follows [2-4]:

$$\Delta P_c(t) = \rho g [h_1(t) - h_2(t) - \Delta h_{st}] \quad (A.6)$$



Sangho Kim received his B.S. degree in Mechanical Engineering from Kyung-Pook National University in 1997. He then received his Ph.D. from Drexel University, USA, in 2002. Dr. Kim is currently an Assistant Professor in the Division of Bioengineering and the Department of Surgery at the National University of Singapore in Singapore.



Dohyung Lim received B.S. and M.S. degrees in Biomedical Engineering from Inje University, Kimhae, Korea, in 1998 and 2000, respectively. He then went on to receive his Ph.D. from the School of Biomedical Engineering, Science, & Health Systems, Drexel

University, Philadelphia, PA, USA, in 2004. Dr. Lim completed a postdoctoral fellowship in the Department of Physical Therapy and Human Movement Science, Feinberg School of Medicine, Northwestern University, Chicago, IL, USA and was a Research Professor of Biomedical Engineering, Yonsei University, Wonju, Gangwon, Korea. Dr. Lim is currently a Senior Researcher at the Korea Institute of Industrial Technology in Cheonan, Chungnam, Korea.